Investigating Potential Mechanisms of Selected Intracellular Metabolites on Preformed Lysozyme Oligomers at Physiological pH*

Abstract

Proteins undergo misfolding due to changes in physiological condition, mutation or cellular homeostasis. Protein misfolding and subsequent amyloid formation results in various neurodegenerative conditions. As disturbed homeostasis of nitrogenous bases and nucleosides are associated with neurodegenerative diseases, we have earlier investigated the effect of these molecules on protein amyloid formation, as reported in Chapter 3. In the current study, we have further investigated the effect of these compounds on preformed amyloid as well as on specific steps of the amyloid formation, including primary nucleation, secondary nucleation and elongation. Our results show that these ligands, converts soluble aggregates/oligomers at physiological pH towards more matured fibrils as measured by Thioflavin T (ThT) binding and atomic force microscopy. Surprisingly, turbidity and UV scattering intensity of the preformed oligomers at physiological pH decrease, which may be due to an overall decrease in scattering due to the presence of large aggregates in the solution. Detailed investigation of ThT binding kinetics showed that these ligands at physiological pH modify key microscopic protein aggregation processes depending on the step of aggregation they are introduced in. While they promote oligomer to mature amyloid formation, fragmentation and elongation are inhibited. The study provides aspects for further investigations of these metabolites as protein aggregation modifiers and potential therapeutics in neurodegenerative diseases.

_____

* Part of the work is submitted for publication

4.1 Introduction:

Correct protein folding is essential to perform various functions and maintain proper cellular homeostasis. In general, the protein folding processes are pretty complex, and often, a lack or malfunctioning of various quality control within a cell can lead to protein misfolding. Accumulating misfolded proteins within a cell enhances the chances of protein aggregation processes which are the primary cause of various systemic and neurodegenerative conditions in humans (Dobson, 2003; Stefani, 2008; Sarkar *et al.*, 2011, Sarkar *et al.*, 2011). Chaperone systems are well evolved within cells to counter such acts of protein misfolding, although sometimes triggered by factors such as ageing, mutations, and changes in the local microenvironment can lead to poor functioning (Dobson, 2003; Stefani, 2008; Sarkar *et al.*, 2011, Sarkar *et al.*, 2011, Chiti and Dobson, 2017). Ordered protein aggregates exhibiting fibrillar structures rich in β-sheet are commonly known as amyloids. Amyloids generated from misfolded protein aggregates cause various diseases like Alzheimer's disease, Parkinson's Disease, Huntington's Disease, Diabetes Type II, Creutzfeldt-Jacob Syndrome, and prion's disease (Dobson, 2003; Stefani, 2008; Ahmed *et al.*, 2010; Sarkar *et al.*, 2011; Chiti and Dobson, 2017; Sengupta *et al.*, 2016). Initial studies hinted that matured amyloid fibrils led to neuronal death and pathogenesis, although since protein aggregation is a complex dynamic procedure that creates multiple intermediates, it is often difficult to single out a particular step. Extensive research has now led to a consensus that there is no direct correlation between the size of the fibrils and toxicity. Further recent studies have also reported that intermediate oligomeric species are more toxic than matured fibrils and, in some instances, matured fibrils are protective compared to toxic oligomeric species (Kayed *et al.*, 2003, Kayed *et al.*, 2006, Kayed *et al.*, 2013, Ahmed *et al.*, 2013, Asai *et al.*, 2015).

Recent investigations have identified important roles of particular purines like adenosine and guanosine as critical molecules playing essential roles in various cellular processes. Adenosine show inhibitory activity against excitatory neurotransmitters acting through the presynaptic A1 receptors, whereas Guanosine administration in rodents in the case of Parkinson's disease models

has shown inhibition towards a decrease in apoptotic cell death. Further, guanosine has also shown the generation of neurons in substantia nigra, and decreased motor problems associated with the condition (Farina *et al.*, 2013; Kundu *et al.*, 2020; Kundu and Dubey, 2021). Besides these purines, monophosphate and triphosphate nucleotides also play essential functions in maintaining homeostasis in the central nervous system. P1 and P2 receptors are present abundantly on various cell surfaces throughout the nervous system for adenosine-based purines (Federico *et al*., 2012; Fasullo and Endres, 2015; Kundu *et al*., 2020). Also, other pyrimidinergic and purinergic molecules like inosine and uridine might have therapeutic potential in the case of various conditions like epilepsy, pain, anxiety, schizophrenia, Alzheimer's and Parkison's Disease (Federico *et al.*, 2012, Ahmed *et al.*, 2014). Drug discovery using endogenous metabolites could be a viable alternative to synthetic drug discovery as they involve higher production costs and rigorous screening and approval processes.

In the current study, we have used hen egg-white lysozyme (HEWL) as a model protein for producing oligomers using pH and temperature as critical factors. The HEWL amyloid/oligomer is very well reported in the literature. Further, we have utilised selected endogenous metabolites belonging to the class of nucleosides and nitrogenous bases to study their effect on modulating the oligomeric state towards a more fibrillar state, potentially less toxic. We have extensively used spectroscopic and microscopic techniques and complementing aggregation kinetics to gain valuable insights into establishing a potential mechanism that the ligands exhibit depending mainly on the dynamic behaviour of proteins based on pH. We have utilised atomic force microscopy (AFM) experiments to monitor morphological changes. Lastly, we performed Thioflvin T kinetics with and without ligands, which gave us valuable insights into understanding the critical molecular steps affecting protein aggregation/amyloid formation.

4.2 Materials and Methods

4.2.1 Materials: We bought Hen Egg White Lysozyme (HEWL), EC 3.2.1.17 in lyophilised form from Sigma (5g). Further, we bought animal cell culture-grade ligands from Himedia. They were

stored at suitable temperatures until used; thioflavin T (RM10365) was procured from Himedia and ANS (A5144) from Sigma. Tris Buffer and all other necessary chemicals used were of analytical reagent grade. Unless mentioned otherwise, we performed all the experiments in triplicates and employed statistical analyses wherever necessary. We took readings thrice at 0hrs, 24hrs and 72hrs, respectively, for Thioflavin T, ANS, Light scattering, turbidity and tryptophan fluorescence experiments.

4.2.2 Preparation of stock solutions: We prepared 50 mM Tris-100 mM NaCl buffer, pH 7.4 and filtered it through a 0.22 µm sartorius filter of 45 mm diameter. The filtered buffer was used to prepare all the other stock solutions. We checked for the UV absorbance of the buffer at different wavelengths, viz. 280 nm, 350 nm and 405 nm. We prepared a 500 µM stock solution of Hen egg-white lysozyme, keeping the working concentration of lysozyme to prepare amyloid fibrils at 50 µM. We prepared the stock solution of ligands at a concentration of 2 mM in the same buffer. The working concentration ratio of the protein and ligands in the overall solution was optimised at 1:10. We stored the stock solutions at 4ºC until usage and did not store them for more than four weeks. We prepared the stock solution every time in a freshly prepared buffer.

4.2.3 Generation of HEWL oligomers: We used Hen Egg-White Lysozyme (HEWL) protein for the current study. For the generation of soluble oligomers in the aqueous phase, we incubated HEWL at a working concentration of 50 µM in a sample volume of 1ml in a shaking incubator at 55ºC, 180 rpm for 120 hours using 50 mM Tris-100 mM NaCl buffer, pH 7.4. After 120 hours of incubation, we added the ligands to their working concentration and made up the volumes so that the ratio of protein: to ligands was 1:10 for every experiment.

4.2.4 Tryptophan fluorescence and fluorescence quenching: We measured the tryptophan fluorescence of the prepared samples with and without ligands excitation at 295 nm and scanned between 305 nm and 400 nm. We observed quenching by all the ligands under working concentrations. We performed quenching experiments with 10 µM protein concentration and ligands concentration ranging from 0.5 mM-4.5 mM for Guanosine, Thymine and Uracil. We

optimised concentrations of Adenosine and Guanine to be between 3 mM-30 mM and Cytosine in the range of 1mM-10 mM in the same manner. We estimated the Stern-Volmer constant (Ksv) and the number of binding sites (n) using the following equations: $F0/F = 1 + KS_V*[Q]$ and $\log((F0/F)/F) = lo(Ka) + n*\log[Q]$. In the equations, F0 is the intensity without ligands, and F is the intensity with ligands at different concentrations (Suthar *et al.*, 2013, Verma *et al.*, 2019).

4.2.5 Endpoint Thioflavin T assay and Thioflavin T kinetics: We utilised Cary Eclipse Varian Fluorescence Spectrophotometer, Agilent Technologies, to monitor the Thioflavin T intensities of the samples. We kept the slit widths for excitation and emission at 5 nm for all spectrophotometric experiments. We prepared a 1 mM stock solution of ThT in 50 mM Tris buffer, pH 7.4, and added 5% sodium azide for proper storage. ThT was freshly prepared for all separate experiments. The entire solution was filtered using a 0.2 μM filter and stored at 4 ⁰C wrapped in an aluminium foil. The ratio of the protein and ThT used for this assay was 1:5. We added 500 μM of Thioflavin T in all the solutions approximately 30 minutes before measuring the fluorescence at room temperature. We scanned the ThT assay from 460 nm-610 nm with an excitation at 445 nm and λmax 483-488 nm (Kumar *et al.*, 2008).

We performed three different thioflavin T kinetics assays in the current study. Firstly, we established the approximate model of HEWL aggregation using a range of concentrations of HEWL from 20 μM, 50 μM, 100 μM, 150 μM and 200 μM 50 mM Tris-100 mM NaCl buffer at pH 7.4. For a mechanistic understanding of the behaviour of ligands and their impacts on various stages of protein aggregation, we measured ThT intensity as a function of time. We performed the experiments in two phases to understand the roles of the ligands in inhibiting key steps such as primary nucleation, secondary nucleation and fibrillation. The first Thioflavin T kinetics was studied by incubating selected intracellular metabolites with preformed HEWL early oligomers at a specific concentration. Secondly, we performed a separate experiment by adding a preformed seed in a 1:1 ratio to a freshly prepared HEWL monomer solution. We sonicated the seed solution for 15 minutes with a pulse of 5 seconds ON and 7 seconds OFF to break down the oligomers formed. We

aimed to understand the impact of ligands on a possible inhibition of secondary nucleation. We normalised the Thioflavin T kinetics raw data using Amylofit– The Amyloid Aggregation Fitter (https://amylofit.com) server developed by Miesl *et al.*, 2016. We also used the Boltzmann equation for calculating our lag times in seeded experiments

4.2.6 Light scattering by protein aggregates: We employed UV visible spectroscopy to estimate the presence of large particles in the protein solution. We scanned the protein samples with and without ligands from 410nm-240 nm for UV spectroscopy measurements. Aggregate free protein samples usually do not show any absorbance beyond 320 nm. We were interested in noting the absorbance between 320 nm-350 nm, exclusively attributed to the scattering of light by large aggregates present in the sample. Further, to understand the contribution and number of aggregates in the solution, we traced the double log plot of absorbance versus wavelength using the equation: where the negative slope of the line is a measure of the number of aggregates and approximate particle size (Ranyal and Lenormand, 2014). We measured the turbidity of the different samples prepared as a function of the absorbance of the solutions at 405 nm. The blanks were appropriately subtracted for all calculation purposes.

4.2.7 Atomic Force Microscopy (AFM): We employed Atomic Force Microscopy imaging to better understand the morphology of HEWL oligomers before and after adding the chosen ligands. We carried out the imaging using NT-MDT Nova Technologies using 10µl of prepared HEWL sample oligomers, both untreated and treated, after 72 hours of treatment. We used freshly cleaned ITO slides as substrates. We applied the samples with 2µl of 10mM Magnesium Chloride for better adherence. After a few minutes, we rinsed the samples with milli Q water. We kept the samples for drying overnight in a dust-free environment (Prabhu and Sarkar, 2022). We collected the AFM images in semi-contact (tapping) mode. The cantilever force constant was 3.5N/m±20%, with a resonate frequency of 140 kHz and a scan rate of 0.5 Hz, 256 lines per second over an area of 10µm * 10 µm. We acquired and analysed the AFM images using NT-MDT software Nova Px (Molecular Imaging and tools for Nanotechnology) v.3.2.5.

4.2.8 Statistical analyses using OriginPro (Learning Edition): We have utilised the OriginPro Learning Edition to perform the statistical analyses and generate the graphs.

4.3 Results:

Protein misfolding diseases result in medical conditions which are often difficult to diagnose due to poor understanding of the various micro-processes that underlie the process. The lack of suitable drugs that could target critical steps in protein aggregation makes these investigations insightful for drug discovery. In the current study, we have made some attempts with important endogenous metabolites as potential anti-amyloidogenic agents on preformed HEWL oligomers under *in-vitro* conditions. Hen egg-white lysozyme readily forms amyloids under specific experimental conditions like high concentration of protein, alkaline or physiological pH, high temperature, and salt concentration as well reported in the literature.

4.3.1 Selected Intracellular metabolites enhance the amyloid formation of HEWL: Our Thioflavin T results indicate the rapid formation of matured fibrils upon adding ligands on preformed oligomeric solutions of HEWL. Similar trend was seen at time points 24hrs and 72hrs as well. The current study is focussed towards understanding the influence of the selected metabolites on key steps of amyloid formation converting oligomeric states to matured fibrils. (Fig 4.1).
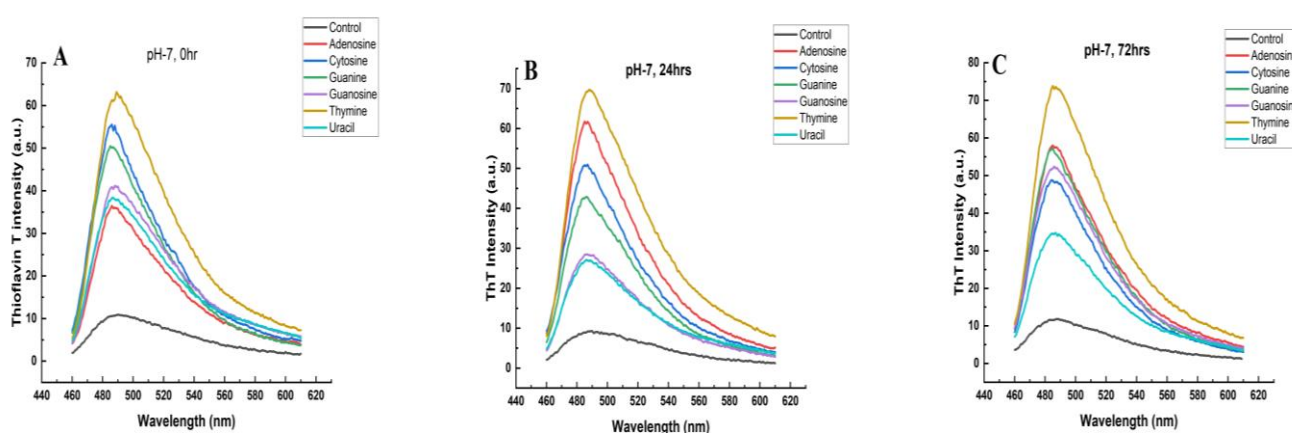

Fig 4.1 Thioflavin T intensity after addition of ligands to preformed HEWL oligomeric solutions: (A) 0 hr **(B)** 24hrs and **(C)** 72 hrs

4.3.2 Atomic Force Microscopy imaging: Our atomic force microscopy images align with our previous results. The histogram analysis of the atomic force microscopy images showed that in the presence of the ligands, the hen egg-white lysozyme showed lower counts in the solution although exhibited an increased height in the range of 200 nm-400 nm. An increase in the height of the samples in the presence of ligands indicates the formation of matured fibrils. An increase in the height of aggregates in AFM and increased Thioflavin T intensity of solutions in which HEWL is present with ligands also supports the finding that the addition of these metabolites in preformed oligomeric solutions escalates the process of fibrillation (Fig 4.2).
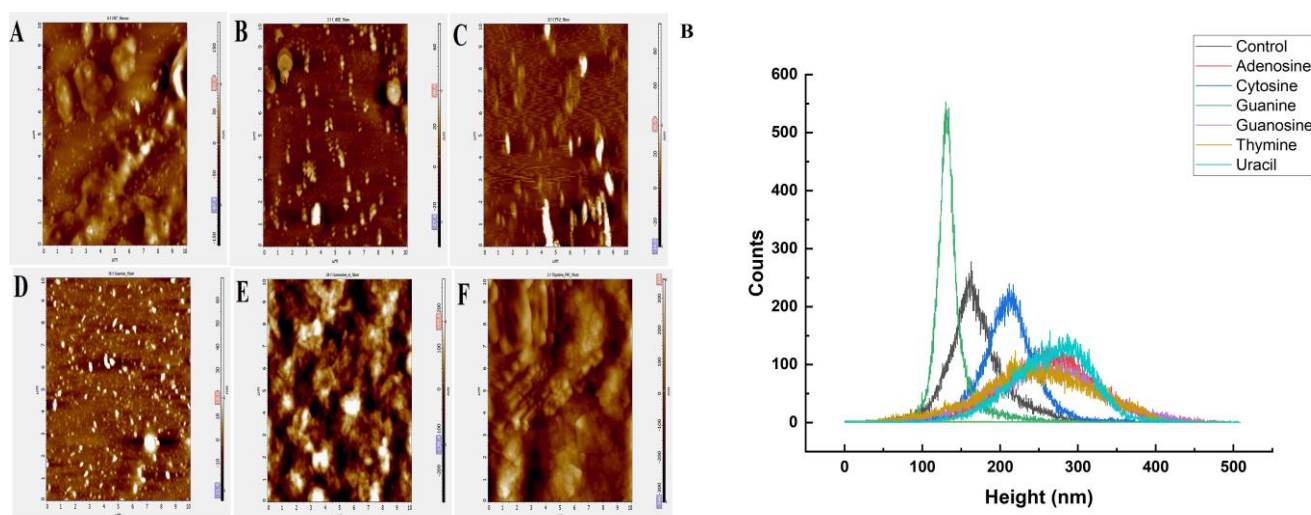

Fig 4.2 Atomic Force Microscopy images (A) Imaging of control sample and various other HEWL solutions in the presence of various ligands and **(B)** Histogram profiling showing the average heights and counts of the various samples

4.3.3 Light Scattering via UV and Turbidity assay: The absorption of protein at 280 nm is majorly dependent upon amino acid composition; as a result, simple absorbance at 280 nm and 340 or 320nm is not a suitable procedure for monitoring aggregation components in protein solutions. In this study, we have used data points between 320 nm-350 nm and plotted a curve to determine the scatter component of the control and treated samples. We used a double log plot curve with absorption values vs wavelength and used the equation: $\log(A) = c - k \cdot \log(\lambda)$. The degree of aggregation, including particle size and population, can be monitored using the k value. The larger

the value of k is, the less aggregated the solution is. We compared the k values at two-time points, 24 hrs and 72 hrs for all the samples. The control sample showed a slight decrease in the value of k at 72hrs compared to 24 hrs. Upon adding ligands, all the systems excluding adenosine showed an increase in the k value at 72 hrs than at 24 hrs in the respective system than control after 72 hours of treatment. The k value indicates that the particle size and population change over time (increase). The increase in k value in the presence of various ligands is explained in section 4.0. With time, uracil and thymine increased k values, indicating changes in the overall aggregated content solutions.

Further, we measured the turbidity of the protein solutions in control and treated samples at three different time points. The ratio of turbidity exhibited at different time points in treated samples decreased over time. The overall turbidity of the untreated HEWL solution increased with time. Compared to control, there was a slight reduction in turbidity of solutions after 24 and 72 hours of treatment. The decrease in turbidity of solutions and scattering intensity between 320-350 nm despite an increase in ThT intensity is an exciting result whose potential reason is described in our discussion section (Fig 4.3).
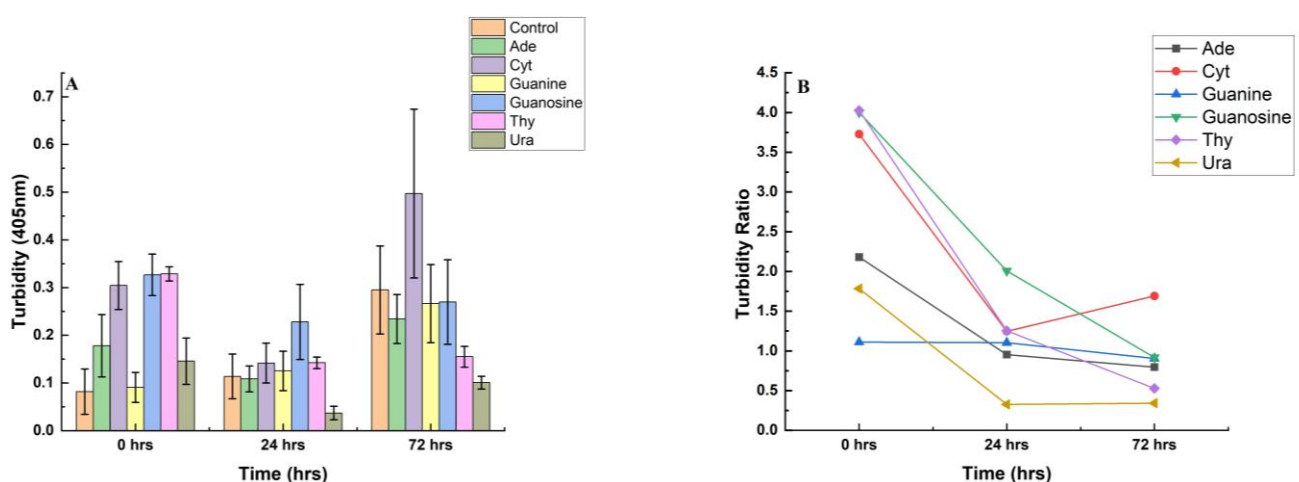

Fig 4.3 Turbidity of various performed HEWL early oligomeric solutions (120 hrs) after addition of ligands at different time points (A) Turbidity at 405 nm and **(B)** Ratio of turbidity of various ligand added solutions with respect to control samples (no added ligands)

4.3.4 Selected Intracellular metabolites quench tryptophan fluorescence of HEWL: Earlier studies have suggested that amyloid-prone regions in proteins have a higher propensity for hydrophobic amino acid residues, especially tryptophan (Pace *et al*., 1995, Sarkar and Dubey, 2010, Ranyal and Lenormand, 2014). Although studies have suggested that HEWL fibrillation is dominated by denaturing conditions (Sarkar and Dubey, 2010), followed by quenching, our studies have shown no significant peak shift of λ max even under experimental conditions, suggesting that for HEWL to form soluble oligomers, prior denaturation is not a mandatory event. Fluorescence quenching is an event that occurs in proteins in the presence of other small molecules. Our study has shown that all ligands at working concentration exhibit fluorescence quenching. Our previous docking studies with these ligands and HEWL have also shown potential hydrogen bonding or other non-covalent interactions with Trp62, 63 and Trp108. Our study validates the interaction of the ligands with tryptophan residues in both amyloid-prone and non-amyloidogenic regions, explaining the current study's quenching.

We employed a separate fluorescence quenching study to evaluate further the Stern-Volmer coefficient and the approximate number of potential binding sites for each ligand. Our results show that all the ligands except guanosine in the Stern-Volmer equation have a typical linear relationship between quencher concentration and fluorescence intensity values in the chosen range of quencher concentration. There is a substantial deviation from the typical linear relationship in the case of guanosine, indicating that both static and dynamic quenching might be in play. Further, it also has the highest Ksv value of $1.74\pm0.048M^{-1}$ with approximately two binding sites (n~2). Thymine (Ksv=$1.03\pm0.052M^{-1}$, n~1.035) and uracil (Ksv=$0.658\pm0.036M^{-1}$, n~0.807) show good quenching exhibiting at least one binding site for each ligand (Fig 2). Higher Ksv values in the case of specific ligands indicate that the tryptophan residues are more accessible to particular than the others. Adenosine, Guanine and Cytosine exhibit low Ksv values. We have shown the results in Table 4.1.

Table 4.1- The approximate number of binding sites and Stern-Volmer Coefficient (KSv) of the various ligands in the current study. The experiments were performed multiple times. A typical experimental data was analysed using Origin 2022b (Student Version). The Ksv values are computed using the standard straight-line equation software to find slope of the equation.

Ligands under study	Binding sites (n)	Stern-Volmer coefficient (KSv)
Adenosine	0.763 ~ 1	0.012±0.0009
Cytosine	1.26	0.179±0.0038
Guanine	0.814 ~ 1	0.08±0.0044
Guanosine	2.02	1.74±0.048
Thymine	1.03	1.03±0.052
Uracil	0.807 ~1	0.658±0.036

4.3.5 HEWL shows a saturating elongation and fragmentation-dominated aggregation pathway at physiological pH: Protein aggregation pathways are complex and comprised of multiple pathways simultaneously. Since it does not follow linear processes, individual processes and their rates play an important role in governing the overall aggregation process. In order to understand the microscopic processes of HEWL aggregation and the way the chosen metabolites affect the aggregation mechanism, we initially aimed to decipher the kind of model HEWL aggregation follows. We performed a Thioflavin T assay under controlled experimental conditions in a range of concentrations of HEWL ranging from 20 μM to 200 μM. When we analysed the raw data for half time with respect to the concentrations, we considered the widely accepted form of power-law $t_{1/2} \sim [m]^{\gamma}$, where γ is the characteristics exponent, which gives us an idea of the dominant nucleation mechanism present (Knowles *et al.*, 2009, Miesl *et al.*, 2014).

We normalised the raw data using the Amylofit online fitting platform and calculated the half-times of the various concentrations. As reported earlier in the case of amyloid β peptide, in the case of Hen Egg White Lysozyme, we also report that the scaling component depends on the concentration range under which the aggregation process is on. In our case, we report that for the range of 20 μM to 100 μM, the scaling component is -0.337, whereas for the range including 20 μM to 150 μM, the scaling component reduces to -0.039. The scaling component (γ), as calculated from our normalised data, for all concentrations (20 μM to 200 μM) was -0.012. The lowering of scaling component with increasing concentration ranges indicated that the model of HEWL aggregation in

the above concentration range was saturating elongation and fragmentation (Miesl *et al*., 2014). The combined $k_n k_+$ rates for the different concentrations of HEWL indicate that a higher rate is observed at low and very high concentrations of the protein, whereas in intermediate concentrations, the $k_n k_+$ rates are a little lower (Fig 4.1). This observation remains to be explored at the end of the study.
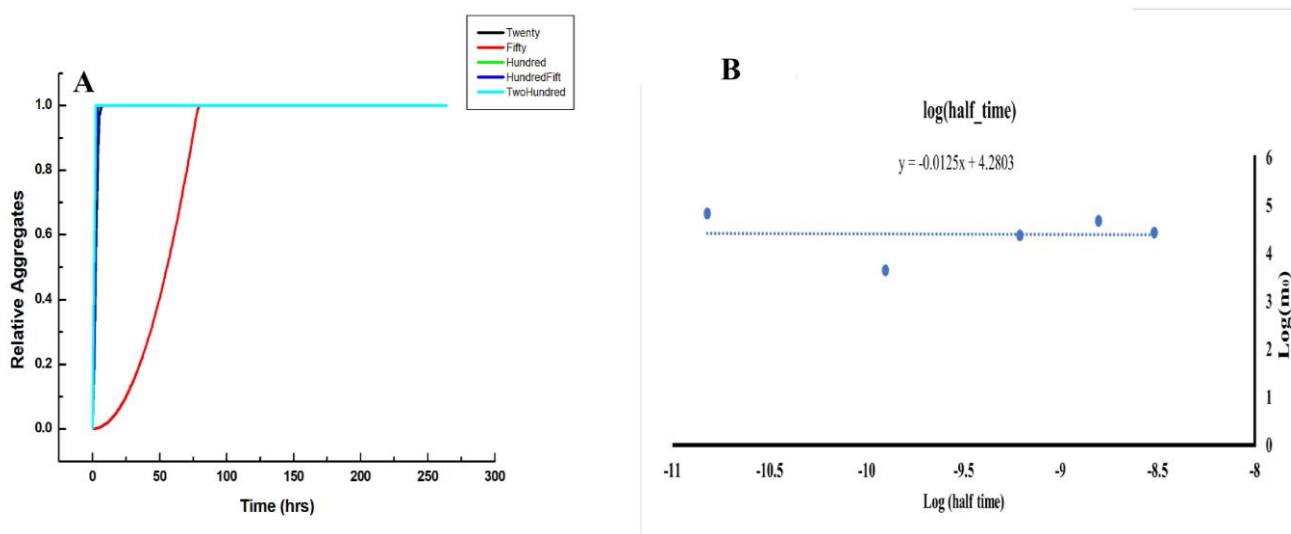

Fig 4.4 Thioflavin T kinetics of HEWL at various concentrations: **(A)** Normalised Relative Aggregate Vs time of various HEWL concentrations computed using the Amylofit server and **(B)** Double Log Plot of half time Vs m_0 indicating the scaling component. The double log plot of Half time Vs m_0 is fitted in a straight line. The slope of the straight line (scaling component) represents the dominating process of the entire aggregation under specific conditions. The scaling component value between 0 to -0.5 represents multiple processes are dominating aggregation. The model of aggregation under such conditions is called as saturating elongation and fragmentation (Miesl *et al*., 2016).
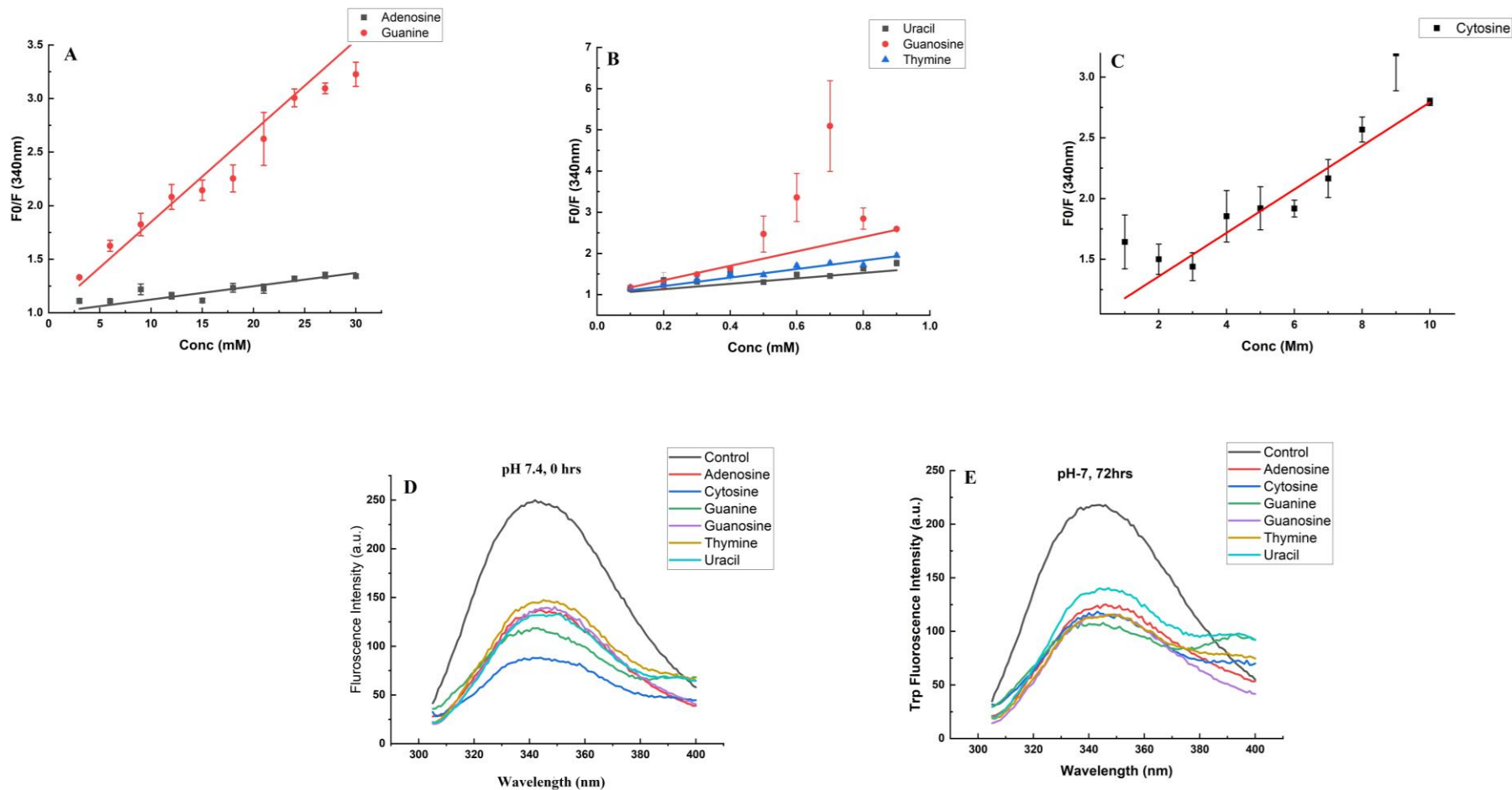
Fig 4.5 Tryptophan fluorescence quenching by various ligands: (A) Stern-Volmer plot of Adenosine and Guanine **(B)** Stern-Volmer plot of Uracil, Guanosine and Thymine **(C)** Stern-Volmer plot of Cytosine **(D)** quenching after 0 hrs of addition of ligands and **(E)** after 72 hrs of addition of ligands

4.3.6 ThT Kinetic Analysis: To better understand the mechanism that the ligands might be exhibiting, we carried a Thioflavin T kinetics assay in the absence and presence of all the ligands at optimal concentration. The aggregation kinetics of the systems mainly exhibited a typical sigmoidal behaviour. Further, we utilised Amylofit- The Aggregation Fitter webserver to fit the normalised data for obtaining the combined rate constants of primary nucleation (k_nk_+) (Miesl *et al.*, 2016). Combined rate constants are more insightful for unseeded reactions than individual rate constants. In the current study, we report that both nitrogenous bases and nucleosides enhance k_nk_+ rates and simultaneously reduce $t_{1/2,}$ implying faster protein fibrillation in the presence of ligands. Thymine reduces $t_{1/2}$ by approximately 54% and increases the k_nk_+ by seven times, followed by Cytosine (50%), guanine (42%) and uracil (33%). Adenosine and guanosine reduce half-time but not as much as the other ligands. Half-time reduction is directly proportional to an increase in k_nk_+ rates (Table 4.2). We report that nitrogenous bases enhance fibrillation more compared to nucleosides.

Table 4.2- The combined k_nk_+ (nucleation and growth) rates for various systems under consideration and the potential mode of action of various ligands in the study, nc is 2.0 used as a global constant for nucleus size, $t_{1/2}$ is the time in which half of the maximum intensity is reached. m0 is the concentration of the starting monomer.

Ligands	m0	nc	k_nk_+ (Mol^{-1} hr^{-1})	$t_{1/2}$ (hrs)	Fold Change	Mechanism
Control	50 μM	2	1.20 E+04	135.64	N/A	
Adenosine	50 μM	2	2.98 E+04	100.64	2.48	Promotion of fibrillation
Cytosine	50 μM	2	7.18 E+04	68.23	5.98	Promotion of fibrillation
Guanine	50 μM	2	5.37 E+04	79.89	4.48	Promotion of fibrillation
Guanosine	50 μM	2	2.14 E+04	113.6	1.78	Promotion of fibrillation
Thymine	50 μM	2	8.69 E+04	63.04	7.24	Promotion of fibrillation
Uracil	50 μM	2	3.77 E+04	91.56	3.14	Promotion of fibrillation

Since amyloid aggregation is an assembly of microscopic processes, including primary nucleation and secondary nucleation, we also wanted to explore the effect of the metabolites on secondary nucleation. We performed a seeded experiment where we added a seed of stock 2mM

concentration incubated at 55 ºC for seven days. Before adding the seed, we sonicated the solution to increasing the protein oligomers' fragmentation before adding the seed. The seed concentration added to the original protein solution was such that the ratio of working concentration of both m_0 (initial monomer concentration) and M_0 (mass concentration of fibril) at the time of seeding is 1:1. In amyloid formation, secondary nucleation strongly influences amyloid progression. In seeded experiments, adding seeds to protein solutions can accelerate the aggregation rate. Our analysis shows that there was not much difference observed in the lag phase period of the control sample (HEWL only) and the samples in which metabolites were present in all the test solutions. In the protein aggregation process dominated by secondary nucleation, shortening of lag phases is a characteristic of adding preformed seeds to aggregating solutions (Fig 4.6B). Our results indicate that our ligands do not influence the secondary nucleation process as there are no significant changes in the overall lag phase of the protein samples in the presence of ligands compared to the control sample (Table 4.3).

Table 4.3- The approximate lag time in hours and potential mechanism of ligands in seeded reaction

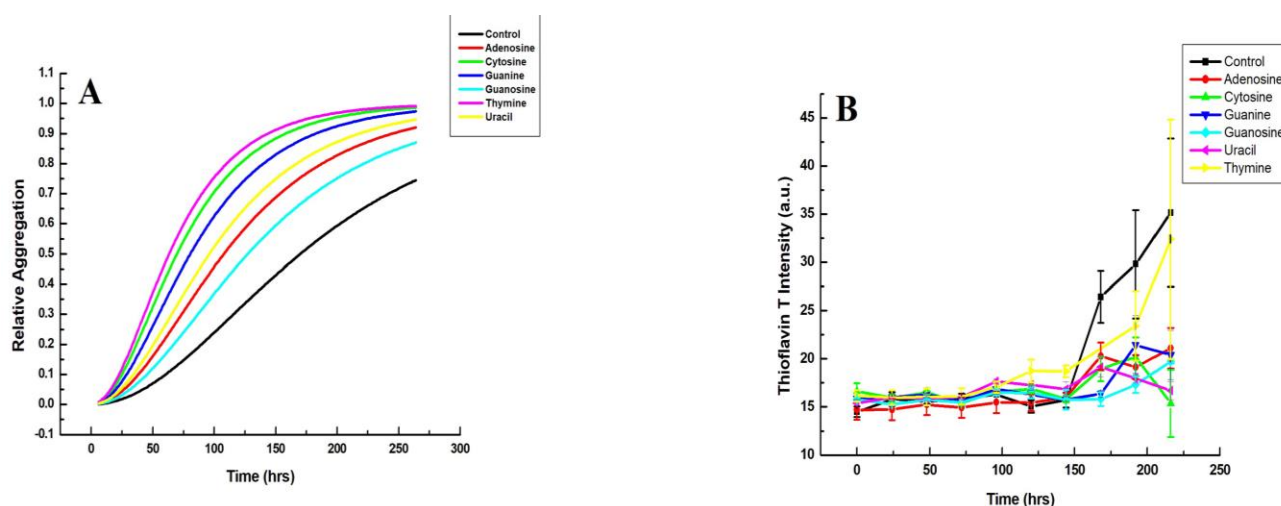| System under study	Lag time (hrs)	Mechanism of action
Control	165.61	N/A
Adenosine	143.53	Secondary nucleation/Elongation Inhibition
Cytosine	165.15	Secondary nucleation/Elongation Inhibition
Guanine	221.5	Fibrillation inhibition
Guanosine	330.78	Fibrillation inhibition
Thymine	471.14	Fibrillation inhibition

Fig 4.6 Thioflavin T Kinetics Analysis: (A) Unseeded HEWL oligomeric solutions and **(B)** Seeded HEWL oligomeric solutions with and without various ligands at desired concentrations.

4.4 Discussion

Amyloid research has made significant progress in the last few decades. It is now understood that the oligomeric stage is the bigger culprit compared to a mature amyloid fibril as thought earlier (Susanian and Bernson, 2020). Protein misfolding and aggregation is a very dynamic process involving the formation of many transient intermediate states, and hence it becomes challenging to identify specific stages associated with the highest pathological contributions. Other than a lack of understanding of the possible mechanisms of various stages of protein aggregation, the development of drugs to treat various stages of disease progression is also a significant lacuna in current research. Most of the few available drugs are majorly used for symptomatic treatment and merely target the underlying cause of the disease. It is hoped that with a better understanding of the various toxic species identified in the protein aggregation process, newer drugs more specific towards various stages could be more helpful in alleviating pathological conditions (Paravastu *et al.*, 2008, Verma *et al.*, 2015). Recent drug development in this field has two major strategies: developing and curating various small molecules that could target various toxic species and interact with them directly. Thus, by interaction, molecules could prevent the formation of oligomers or fibrils (Lambert et al., 1998) or interact with protofibrillar and matured fibrillar states and destabilise them (Nimmrich *et al.*, 2008).

In the current study, we further explored selected intracellular metabolite's more specific role in protein amyloid formation/dissociation. Our Thioflavin T results indicate an escalation of the fibrillation process as soon as ligands are added to preformed solutions. We observed similar results even after 24 and 72 hours of addition of ligands. Although there was an increase in Thioflavin T intensity, the overall turbidity at 405nm and scattering intensity (320-350nm) of the HEWL solutions decreased with time after adding ligands. A possible explanation is that different regions within large protein aggregates experience a difference in the incident's light electric field, producing a large superimposition of complex scattered light with an overall decrease in the scattering intensity. Further, there is also a decrease in the overall intensity of light as it passes through the aggregate. This is the primary potential reason why the slope of the linear plot of scattering intensity between 320-350 nm increased with time indicating higher overall aggregation in the presence of ligands (Bohren and Hoffman, 2008, Kerker, 2013, Zhao *et al.*, 2016). We observed a similar result in our AFM data which showed a slight increase in both the average counts and the overall height of the sample compared to the control sample. As reported in several other studies, the formation of matured fibrils is coupled with an increase in both height and width of the sample (Hill *et al.*, 2009).

Other than the endpoint studies, we have also examined the very fast fibrillation of oligomers upon the addition of ligands in our Thioflavin T kinetic studies. It is important to note that HEWL follows a saturating elongation and fragmentation model of amyloid formation. This is important for us to understand so that we can identify where in these microscopic processes can our molecules exhibit much impact. Previous studies as well as here, we have shown that the scaling component measured varies as function of the range in concentration used. This also indicates that there are multiple steps taking place in the overall protein aggregation process. Literature shows that such saturation processes are also typical for elongation steps in other proteins (Esler *et al.*, 2000, Knowles *et al.*, 2007). Our kinetic studies with various ligands at a specific concentration of both HEWL and respective ligands showed that they increase the combined rate of nucleation and

fibrillation in unseeded reactions. The results suggest that the ligands are more effective in binding with HEWL at the early oligomeric stage, thus bypassing the formation of toxic oligomers. However, there was no impact on the lag phase of the aggregation process in seeded experiments where we added preformed fragmented oligomers to native HEWL monomers. In fact, adding specific ligands increased the overall lag phase of aggregation and finally reduced overall elongation. This result suggests that the impact of ligands is much related to the protein aggregation stage they experience. The overall kinetic studies concluded that the ligands are more impactful at the early stages of pathology.

Druggability is found in many small molecules and chaperons. Here, we selected nucleosides and Nitrogenous bases as these molecules are endogenous and would not show much toxicity within the nervous system. The challenge arises in understanding the exact kinetics of these micro-processes as no step here is ordered and timed. Small molecules like adenosine and guanosine shows satisfactory potential as protein aggregation modifying agents using Hen Egg-White Lysozyme. The overall processes were studied using established experimentation methods like Fluorescence Quenching which helped us conclude the binding affinity and binding sites of these molecules within the protein. The quenching result also indicates the capacity of the ligands to interact with the K peptide region of the protein consisting of key Trp residues. The quenching of the protein and simultaneous increase in ThT intensity upon addition of ligands indicates that the quenching is possibly due to the interaction of metabolites with Trp residues which might not be necessarily in the amyloid-prone regions. ThT fluorescence revealed that both nucleosides and nitrogenous bases reduce the half time and increase the overall fibrillation, which indicates the process is directed more towards shifting from cytotoxic oligomeric species to stable elongated fibrils. We also studied the overall effect of drugs in seeded reactions (secondary nucleation), in which majority of the metabolites increased the lag phase time and two metabolites did not impact the lag phase significantly. The observation also suggests the potential of these metabolites to slow

down secondary nucleation processes. The increase in size was further validated using atomic force microscopy, in which it was visible that overall fibrillation increased in the presence of ligands.

The study has the potential to act as a link for further studies on Hen egg-white lysozyme aggregation mechanisms. The importance of Hen egg-white lysozyme fibrillation in physiological pH is relevant because it shares high homology with human lysozyme. Human lysozyme is also associated with systemic amyloidosis caused due to various mutations. These intracellular metabolites' impact is a first attempt at studying the direct interaction capability with aggregation-prone protein zones. Computational and biophysical approaches based on the potential of small molecules to directly interact with aggregation hotspots is a novel mechanism now being used extensively to develop drugs for protein misfolding diseases. This strategy can also be extrapolated further to understand the exact mechanisms dependent on a series of concentrations and hence more physiological relevance of these molecules.

4.5 Conclusion:

Ideally, protein misfolding and aggregation have three key steps: primary nucleation, secondary nucleation, and elongation. Much of the drugs discovered to treat various proteinopathies are based on targeting primary, secondary nucleation or elongation of aggregated proteins. Elongation results in matured fibrils consisting majorly of the beta sheets. In the current study, we have used preformed oligomers as therapeutic targets. We aimed at understanding the mechanistic behaviour of some selected metabolites at various stages of protein aggregation. One of the primary observations included the rapid conversion of early oligomers towards a more matured fibrillation which suggested promotion of elongation as the key mechanism. Once we determined the overall model of HEWL aggregation, it was also important to see the effect of these metabolites onto seeded reactions. The observation of increasing lag time in presence of majority of the metabolites indicates possible delay of the progression of the amyloidogenic states which is also of an important strategic and therapeutic potential. The overall process is quite complex to understand how the monomers fold and form amyloid beta-sheets. The experimental process like fluorescence

spectroscopy using dyes like Thioflavin-T and ANS, UV Spectroscopy, and Atomic Force Microscopy help us identify the exact state and progress of these microscopic events and how ligands are interacting and modulating the overall aggregation kinetics. This study provides a robust platform for more rigorous future experiments based on these molecules.